



RSI Technical Note 028

Calculating the Rate of Dissipation of Turbulent Kinetic Energy

Rolf Lueck

2016-05-03

Rockland Scientific International Inc.

520 Dupplin Rd

Victoria, BC, CANADA, V8Z 1C1

www.rocklandscientific.com

Contents

1	Introduction	2
2	The Velocity Shear Spectrum	3
3	The Air-foil Shear Probe	5
3.1	Example shear spectra	6
4	The Nasmyth Empirical Spectrum	10
4.1	Exploiting the Nasmyth spectrum	13
4.1.1	Recursive estimation of ϵ	15
4.2	A note on integration	16

List of Figures

1	Shear Probe	5
2	Shear Probe	6
3	Shear Spectrum in a tidal channel	7
4	Shear Spectrum in a pond – surface mixing layer	8
5	Shear Spectrum in a pond – thermocline	9
6	Nasmyth spectrum – logarithmic form	10
7	Nasmyth spectrum – linear form	11
8	Quality of fit to the integral of the Nasmyth spectrum.	12
9	The inertial subrange.	12
10	The dimensional Nasmyth spectrum.	13
11	ϵ/ϵ_{10} as a function of ϵ	14
12	ϵ/ϵ_{10} as a function of ϵ_{10}	14
13	Quality of the fit of ϵ/ϵ_{10} to ϵ_{10}	15

List of Tables

1	Fraction of Variance	10
---	--------------------------------	----

1 Introduction

This document describes a method for calculating the rate of dissipation of turbulent kinetic energy (TKE) from the shear measured with an air-foil type shear probe.

A new method is presented for several reasons. In the early days of oceanic turbulence measurements the amount of data collected on a cruise was limited – usually to a few dozen profiles. The estimation of the rate of dissipation from shear probe data was only partially automated and required considerable checking and adjusting. This was acceptable because the number of estimates were small. We now have autonomous instruments that can collect shear probe data for many months and this has increased the volume of data by many factors of 10. It is no longer practical to check every spectrum, and the process must be automated by algorithms of high-reliability and must provide enough diagnostic information to flag potentially erroneous estimates.

Before the turn of the century, oceanic turbulence was conducted by only a small number of research groups who each developed their own methods of calculating the rate of dissipation of TKE. There have been some inter comparisons by these research groups, but the statistical nature of ocean turbulence makes these comparisons difficult. Basically, it has been assumed that these research groups derived good estimates because ocean turbulence was their area of expertise and that they were highly dedicated to "doing it right". The number of researchers using the shear probe has increased greatly and the level of expertise of the users of the shear probe now has a far larger range than it did in the last century. In fact some researchers now would not consider themselves experts – for them, the rate of dissipation of TKE provides the background for the study of biological and chemical processes. Because of the proliferation of shear probe users, there is a pressing need to develop a "standard". Although some might argue that a standard method is dangerous because it might contain flaws, the standard is still useful because, if flaws are found, they are quickly and universally rectified if there is a standard method.

Section 2 presents a short summary of the theoretical foundation of the shear spectrum of turbulence and can be skipped by those familiar with this topic.

The shear probe is presented in section 3, along with some sample spectra, and this too can be skipped by those that are already familiar with the shear probe.

I re-examine the Nasmyth spectrum in section 4 and present some of its key properties that will be exploited in the new method of calculating the rate of dissipation of TKE.

2 The Velocity Shear Spectrum

There is no formal definition of turbulence. Instead, it is described as a syndrome with key characteristics, which together, distinguish it from non-turbulent fluid motions. The key characteristics are [1];

- The flow is chaotic or highly irregular or random.
- The flow is rotational – it has three-dimensional vorticity.
- The flow is dissipative – kinetic energy is irreversibly lost through friction.
- The flow is diffusive – causing rapid mixing of fluid properties such as momentum, heat, and other scalar properties.
- The flow is non-linear and transports energy from large-scale eddies to small-scale eddies.
- The flow has a high Reynolds number.
- Turbulent flows are a continuum – the size of the smallest eddies is still many factors of 10 larger than any molecular length scale.

Turbulence is a characteristic of a *flow* and not of a *fluid*. There are non-turbulent flows that have some but not all of the above-listed characteristics. For example, surface waves can be highly irregular but the water motions induced by surface gravity waves are irrotational. Surface waves are highly linear until they grow to the verge of breaking. Then, they can induce considerable turbulence into near-surface water.

Turbulent flows are dissipative. Kinetic energy is transferred from the large-scale background flow into the turbulent fluctuations of velocity by flow instabilities. This creates large eddies with scales comparable to the background. The size of these eddies is either limited by the distance to the boundaries of the flow, or by the stratification of the flow.

Shear instability is a common mechanism that transfers kinetic energy from the mean flow to the turbulence. The rate of production of TKE, in a vertically sheared flow, is

$$-\overline{u'w'}\frac{\partial U}{\partial z} \quad (1)$$

where $-\overline{u'w'}$ is the Reynolds stress and $\partial U/\partial z$ is the mean (background) shear. That is, the Reynolds stress works against the mean shear to produce turbulent kinetic energy.

Vortex–vortex interaction and pressure–velocity correlations break the largest eddies into a cascade of smaller eddies. These motions are non-dissipative – the TKE simply flows to ever smaller scales without any loss of energy. At some point in this cascade, the eddies are small enough to be damped by molecular friction, and this removes the TKE irreversibly and converts it into heat. By dimensional analysis, this scale should be of order

$$\eta = (\nu^3 \epsilon^{-1})^{1/4} \quad (2)$$

where ν is the kinematic molecular viscosity and ϵ is the rate of dissipation of turbulent kinetic energy. In a stationary and unstratified flow, the rate of dissipation equals the rate of production (1). In a stratified flow, approximately 20% of the production goes into raising the potential energy of the fluid – the remainder is dissipated.

The spectrum of the turbulent velocity fluctuations was first derived by Kolmogorov [2], under the assumption that the largest scales of the turbulence (the so called “energy-containing” scales) are much larger than the “dissipative” scales (2). The dissipation scale is now commonly called the Kolmogorov scale. For wavenumbers large compared to the energy-containing range *and* small compared to the dissipation range, Kolmogorov showed that the velocity spectrum must be proportional to $k^{-5/3}$, where k is the wavenumber. This wavenumber span is usually called the “inertial subrange” because the velocity fluctuations are unaffected by viscosity within this range of wavenumbers – the TKE is only passed through this range of wavenumbers without loss.

The form of the velocity spectrum for wavenumbers comparable to and larger than η^{-1} – the range affected by viscosity – was not predicted by Kolmogorov. An empirical spectrum of velocity fluctuations was derived by Nasmyth [3]. Oakey [4] formally published the Nasmyth empirical spectrum and also converted it into the spectrum of the rate-of-strain and shear, under the assumption of isotropic turbulence. The Oakey-tabulated shear spectrum is hereafter referred to as the “Nasmyth” spectrum. Shear (and the rate-of-strain) are the gradient of velocity and, consequently, their spectra rise in proportion to $k^{1/3}$, in the inertial subrange (Figure 6).

In isotropic turbulence, the rate of dissipation of TKE is

$$\epsilon = \frac{15}{2}\nu \overline{\left(\frac{\partial u}{\partial z}\right)^2} = \frac{15}{2}\nu \int_0^\infty \Psi(k)dk \quad (3)$$

where Ψ is the spectrum of the shear, $\partial u/\partial z$. Equation (3) applies equally to any of the other five components of shear ($\partial v/\partial x$, $\partial w/\partial x$, $\partial u/\partial y$, $\partial w/\partial y$, and $\partial v/\partial z$). Equation (3) also applies to the three components of the rate-of-strain, $\partial u/\partial x$, $\partial v/\partial y$, $\partial w/\partial z$, but the numerical scale factor is increased from 15/2 to 15.

3 The Air-foil Shear Probe

The shear probe (Figure 1) was originally developed for wind tunnel work [5] [6] and was adapted for oceanic measurements by Osborn [7]. The air-foil shear probe senses velocity fluctuations cross-stream to its direction of travel. If there is an average axial velocity, W , past the probe, then a cross-stream fluctuation, u , creates an instantaneous angle of attack, α . This angled flow elevates the pressure on the incoming side and reduces it on the outgoing side. The net force is sensed by a piezo-ceramic beam (Figure 1, red) that is cantilevered from the stainless-steel probe sting. The resultant strain produces an electric charge that is proportional to the cross-stream fluctuation times the mean axial velocity, namely uW . It does not matter if the probe is moving through the water (such as when it is mounted on a vertical profiler) or if the probe is stationary and the ambient current moves the water past the probe (such as when it is mounted on a mooring). However, the along-axis velocity, W , should be fairly constant, over the time scale of an individual dissipation estimate, and the angle of attack, α , should be less than 20° . This means that W should be more than 3 times larger than the magnitude of the peak cross-stream fluctuations, u . Because the sensing element is a piezo-ceramic beam, the probe can only detect the fluctuations of cross-stream velocity with a lower frequency limit of about 0.1 Hz.

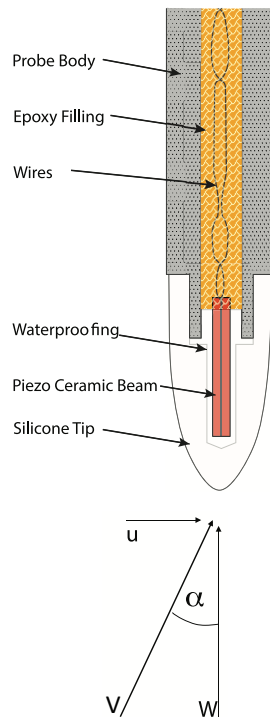


Figure 1: A schematic of the air-foil shear probe in a vertical configuration (discussion below).

A bullet-shaped shroud of silicon rubber surrounds the piezo-ceramic beam to turn the probe into an “air-foil of revolution”. The sting is mounted into the nose-cone (or leading edge) of an instrument such that the flow past the probe is primarily axial. When two probes are mounted on a vertical profiler, they can sense the vertical gradient of each component

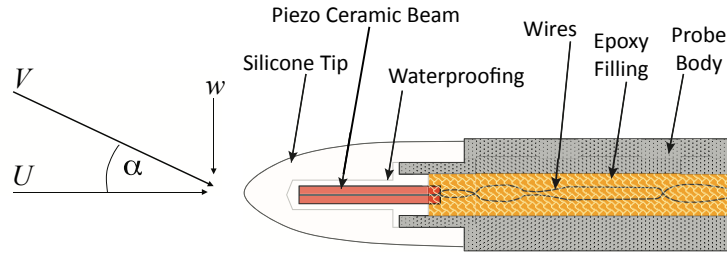


Figure 2: A schematic of the air-foil shear probe in a horizontal configuration.

of horizontal flow, namely $\partial u/\partial z$ and $\partial v/\partial z$. When they are mounted on a horizontal profiler, such as a mooring, the probes can sense, $\partial v/\partial x$ and $\partial w/\partial x$. When a pair of probes are mounted on a glider which travels with a considerable inclination, they would sense $\partial v/\partial s$ and $\partial w/\partial s$ where s is the direction of travel. The velocity components v and w are orthogonal to s . Regardless of the direction of travel, the rate of dissipation of TKE in isotropic turbulence is given by (3).

The finite size of the probe causes it to spatially average the velocity fluctuations when the eddies are comparable to the width of the probe, The half-power wavenumber response is 48 cpm (cycles per metre) according to [8] and takes the form

$$H(k) = \frac{1}{1 + (k/48)^2} . \quad (4)$$

The shear probe is calibrated by the method of [7] to an accuracy of 5%.

3.1 Example shear spectra

The rate of dissipation of TKE takes a very wide range in the ocean. An example of a very large rate of dissipation of TKE comes from a tidal channel in Scotland (Figure 3).

The data were collected in the depth interval of 48 to 55 m, with a vertical free-fall profiler descending at a speed of 0.84 m s^{-1} . The spectra have been corrected for the wavenumber response of the shear probe. However, the anti-aliasing filters in the data acquisition system were set to 98 Hz and limit the resolution to 116 cpm. For this reason, the rate of dissipation is estimated from the level of the spectra in the inertial subrange. The shear signal is so strong that the vibration, and other spurious motions, of the profiler have no signature.

An example of a moderately high rate of dissipation of TKE comes from a 20 m-deep pond on Cape Cod, Massachusetts, USA, using data collected with a Slocum glider while it descended through 7 m-deep surface mixing layer (Figure 4).

The glider was travelling with a speed of 0.28 m s^{-1} and the data were collected in the depth range of 2 to 6 m. The original shear spectra have a high and narrow spike near 100 cpm induced by the pump of the CTD on the glider. The accelerometers in the measurement package (a MicroRider-1000) detect the pump-induced vibrations. The vibration-coherent

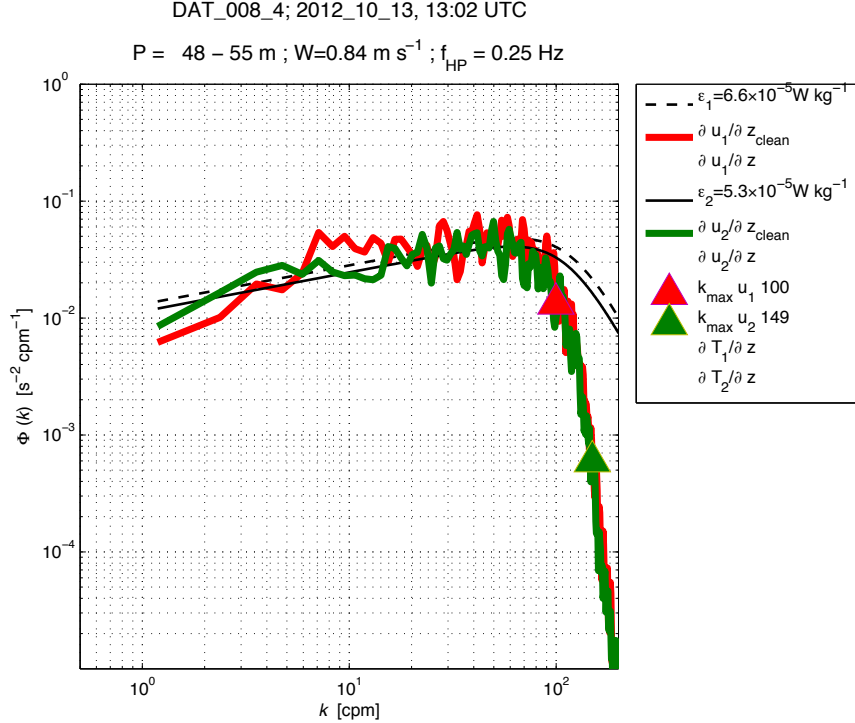


Figure 3: The spectra of two orthogonal components of the vertical shear of horizontal velocity (thick red and green lines). The dimensional Nasmyth spectra are the solid and dashed black lines, for the estimated rate of dissipation of TKE of $\epsilon_1 = 6.6 \times 10^{-5}$ and $\epsilon_2 = 5.3 \times 10^{-5} \text{ W kg}^{-1}$ from shear probes 1 and 2, respectively.

portion is removed from the spectra using the technique of Goodman et al [9]. The spectra rise for wavenumbers larger than about 130 cpm and this is due to electronic noise and vehicular vibrations that are not detected by the accelerometers. The algorithm, used for this example, tries to detect the spectral minimum using a low-order polynomial fit (Figure 4, red and green dashed lines) and, in this case, over estimates the wavenumber of the minimum only slightly (Figure 4, coloured triangles). The estimate of the spectral minimum is used to set the upper limit of integration of the spectrum. This reduces the contribution of noise in the estimate of the rate of dissipation and is a common technique. This technique was used by Osborn for the first data collected with the shear probe and has been adopted by all researchers that use the shear probe. The level of the spectral minimum is 100 times lower than the peak of the spectrum which shows that this is a very well resolved spectrum.

An example of a very low rate of dissipation is provided by the same Slocum glider when it descends into the thermocline below the surface mixing layer (Figure 5). The wavenumber of the spectral minimum has moved to 10 cpm and the polynomial fit provides a good estimate of the wavenumber of the minimum. We find that the method gives good estimates at a rate of more than 90 %, but it is fallible for several reasons. The spectral noise is instrument dependent and the order of the polynomial must be customized to an individual instrument. For the glider, a third- or fifth-order polynomial works well. Other instrument may require an even-order polynomial. Setting the order too high causes spurious and multiple estimates

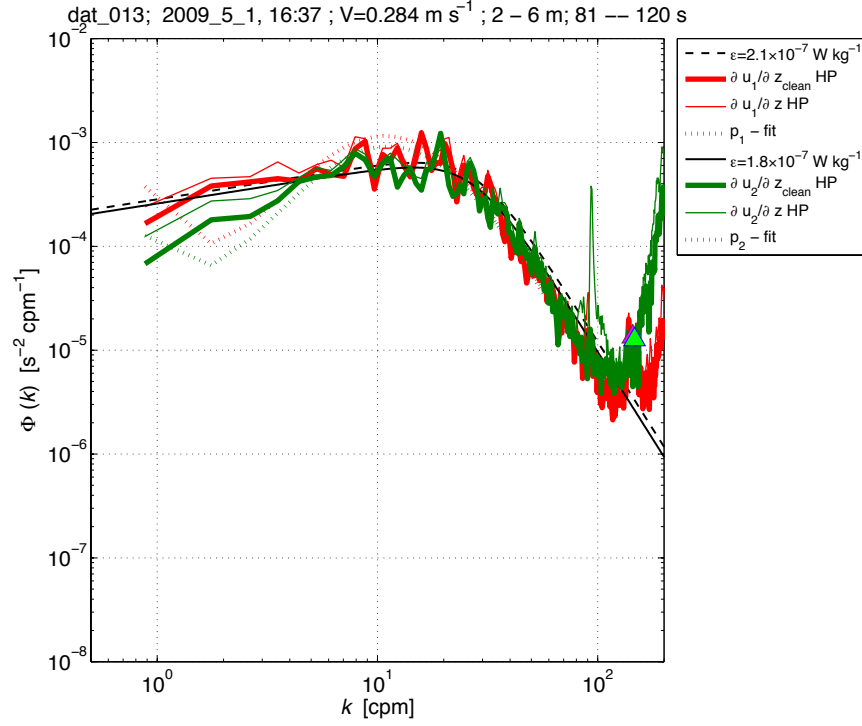


Figure 4: The spectra of two orthogonal components of the (quasi-horizontal) along-path shear (thick red and green lines). The thin solid red and green lines are the spectra before coherent noise removal. The dimensional Nasmyth spectra are the solid and dashed black lines, for the estimated rate of dissipation of TKE of $\epsilon_1 = 2.1 \times 10^{-7}$ and $\epsilon_2 = 1.8 \times 10^{-7}$ W kg $^{-1}$ from shear probes 1 and 2, respectively. The dashed coloured lines are a low-order polynomial fit used to estimate the wavenumber of the minima of the spectra.

of the minima.

The broadband and spectrally rising noise at wavenumbers larger than 10 cpm is large relative to the true environmental shear signal, located below 10 cpm. Without the selectivity of a band-limited estimate of the variance, the rate of dissipation of TKE would have been significantly over-estimated. The level of the spectral peak is only 10 times higher than the spectral minimum. The signal-to-noise ratio is ~ 10 and determines the minimum rate of dissipation resolvable by the shear probe using the current version of its electronics.

Estimation of the shear spectrum involve several considerations and compromises. A common practice is to chose a minimum fft-length that resolves the lowest wavenumber of interest. Typical lengths are 0.5 to 2 m. The smallest wavenumber in the spectrum equals the inverse of the fft-length. When the rate of dissipation is large (such as in Figure 4), the fraction of the variance residing at wavenumbers below 2 cpm is small and a fft-length longer than 0.5 m is not necessary. When the rate of dissipation is extremely small (Figure 5) the fraction of the variance at wavenumbers smaller than 2 cpm is significant, and an fft-length of 2 m is prudent. This example used an fft-length of 1.6 m. The spatial resolution of the dissipation estimates is related to the fft-length. The rate is usually determined from the ensemble average of several (usually 50 % overlapping) fft-segments. Each fft-segment contributes 2 degrees of

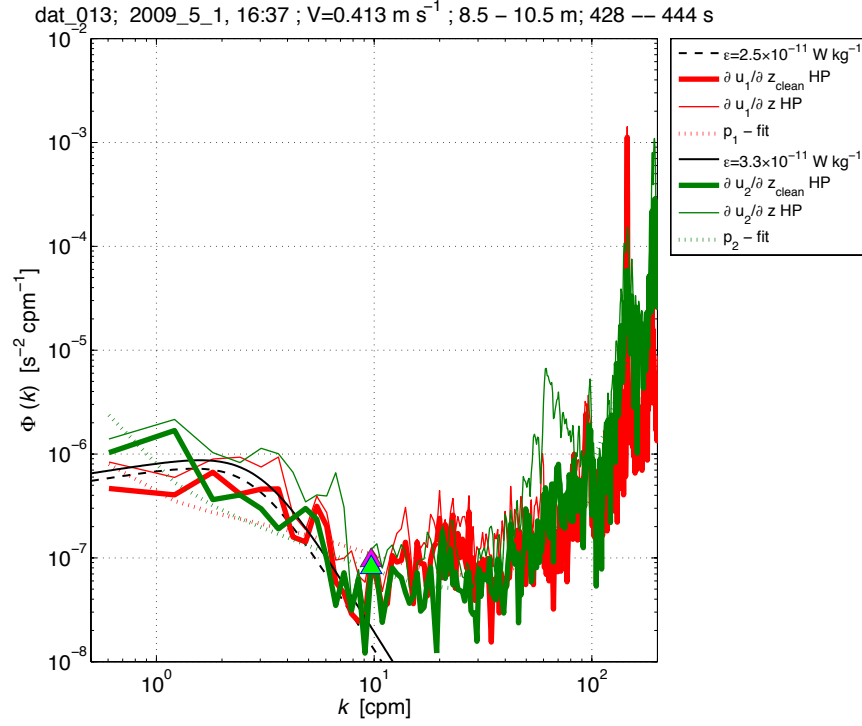


Figure 5: Same as Figure 4, but for data from the thermocline. The rate of dissipation of TKE is estimated at $\epsilon_1 = 2.5 \times 10^{-11}$ and $\epsilon_2 = 3.3 \times 10^{-11}$ W kg $^{-1}$ from shear probes 1 and 2, respectively.

freedom to the approximately χ -square distribution of a spectral value. Three fft-segments should be considered the absolute minimum for reliable estimation. For an estimation that is based on only 3 fft-segments, the degrees of freedom of each spectral point is 6 and the spatial spacing of the dissipation estimates is two times the fft-length. If the spectrum is integrated to 10 cpm, then the total degrees of freedom in the dissipation estimate ranges from 30 to 120 for fft-lengths of 0.5 to 2 m, respectively. A more important concern is the Goodman coherent noise reduction algorithm. The statistical reliability of the coherence estimation improves with degrees of freedom. If there is significant vibrational noise in the spectrum, then this should be the first concern. Good noise removal dictates larger ensembles and, consequently, a lower spatial resolution of the dissipation estimates. The compromise is between spatial resolution of the rate of dissipation, its statistical reliability, noise removal, and the scientific objects of the measurements. This compromise must be made by the user.

Thus, a robust algorithm for estimating the rate of dissipation of TKE must cope with a wide range of values (more than 1 to 1×10^7), respect the wavenumber limitations of the shear probe, and effectively eliminate spurious noise from the estimation of shear variance by integrating the spectrum only up to a well-chosen wavenumber limit.

4 The Nasmyth Empirical Spectrum

The non-dimensional form of the Nasmyth spectrum is tabulated at 13 different non-dimensional wavenumbers, $k\eta$, by Oakey [4] where k is in units of cpm and η is given by 2. This spectrum is shown in logarithmic and linear coordinates in Figures 6 and 7, respectively. The $+1/3$ (inertial subrange) is clearly visible and the eighth value seems to be anomalous (green asterisk enclosed by a red circle). The ninth value is near the peak of the spectrum and for higher wavenumbers, the spectrum drops rapidly due to dampening by molecular viscosity.

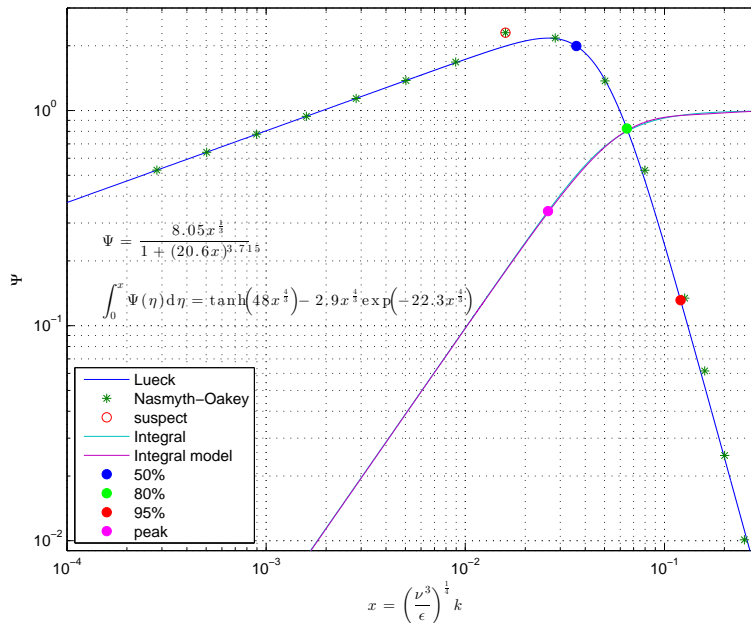


Figure 6: The non-dimensional Nasmyth empirical spectrum of shear (green asterisks) and its mathematical fit (blue). Fifteen-halves times the integral of the Nasmyth spectrum (cyan) and its mathematical fit (magenta). The points where the integral reaches 50, 80 and 95% of its final value are indicated by blue, light-green and red circles, respectively. The peak of the spectrum is indicated by the magenta circle.

	$x = k \left(\frac{\nu^3}{\epsilon} \right)^{1/4}$	Fraction
x_{50}	0.0361	0.50
x_{80}	0.0648	0.80
x_{85}	0.0744	0.85
x_{90}	0.0894	0.90
x_{95}	0.121	0.95
x_{99}	0.232	0.99

Table 1: Fractional variance under the non-dimensional Nasmyth spectrum for non-dimensional wavenumbers x , where k has units of cpm.

Approximately 35% of the shear variance resides with wavenumbers smaller than the spectral peak. 80% of all variance resides at wavenumbers smaller than the point at which the

spectrum has dropped by a factor of 2.7 below its peak. When the spectrum has dropped by a factor of 10 below its peak, it contains (up to this wavenumber), more than 90 % of all shear variance.

Wolk et al [10] provided a mathematical model of the Nasmyth spectrum. The model is not based on physics and is merely a simple mathematical equation that fits well to the tabulated values of the Nasmyth spectrum. By definition, the integral of the non-dimensional shear spectrum, from zero to infinite wavenumber, must equal 2/15. The integral of the model [10] is larger than this value by 4 %. This error has no practical consequences because the 5 % calibration error of the shear probe leads to a 10 % error in the estimate of the rate of dissipation, and there are other errors of even larger magnitude, such as the statistical uncertainty of an estimate from a limited length of data. However, for the sake of consistency, I have revised the model of [10] slightly to bring the integral of the mathematical model of the Nasmyth spectrum to within 0.05 % of its expected value of 2/15. This model is the blue curve in Figures 6 and 7, and is given by

$$\Psi = \frac{8.05x^{1/3}}{1 + (20.6x)^{3.715}} \quad (5)$$

where $x = k\eta = k(\nu^3/\epsilon)^{1/4}$ and the wavenumber k is in units of cpm.

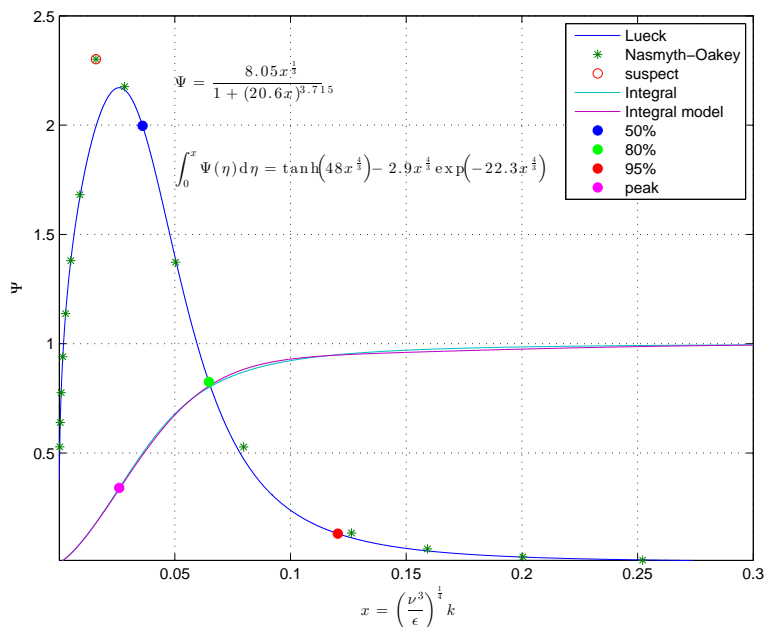


Figure 7: The non-dimensional Nasmyth empirical spectrum in linear space. Markings as in Figure 6.

The integral of the mathematical model is not easily derived by analytic means. The numerical integration of the new mathematical model of the Nasmyth spectrum is the cyan curve in Figures 6 and 7. A mathematical model to the integral of the Nasmyth spectrum is shown in magenta and is given by

$$\frac{15}{2} \int_0^x \Psi(\xi) d\xi = \tanh(48x^{4/3}) - 2.9x^{4/3} \exp(-22.3x^{4/3}) . \quad (6)$$

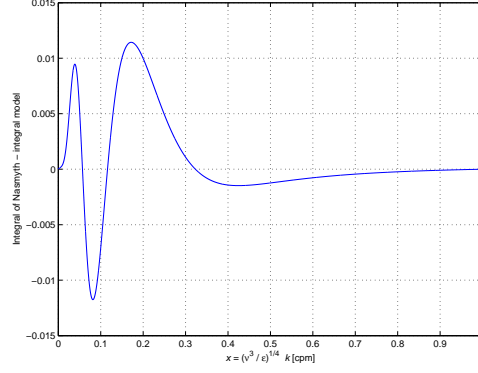


Figure 8: The model of the integral of the Nasmyth spectrum (6) minus the integral of the model of the Nasmyth spectrum (5), when the spectra are normalized to an integral of 1 at $x = \infty$.

This model (6) of the integral of the Nasmyth spectrum fits the actual integral of the mathematical model of the Nasmyth spectrum (5) to within 1.1% (Figure 8).

The spectrum taken in the Scottish tidal channel (Figure 3) barely resolves the peak of the spectrum. If the rate of dissipation had been estimated from the variance of shear, then this estimate would have been too small by a factor of 3. The spectrum taken with the glider in the surface mixing layer (Figure 4) resolves the variance to better than 98% (by integration to 150 cpm), while the spectrum from the thermocline (Figure 5) resolves about 92% (by integration to 10 cpm).

The inertial subrange of the shear spectrum can be delineated by dividing the Nasmyth spectrum by $8.05k^{1/3}$ because the resulting curve will be flat (frequency independent) and equal to 1 within this range (Figure 9).

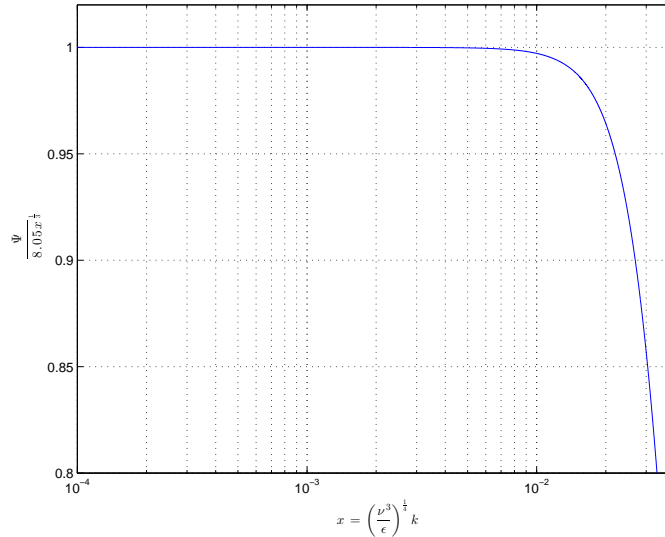


Figure 9: The Nasmyth spectrum divided by $8.05x^{1/3}$ to delineate the inertial subrange.

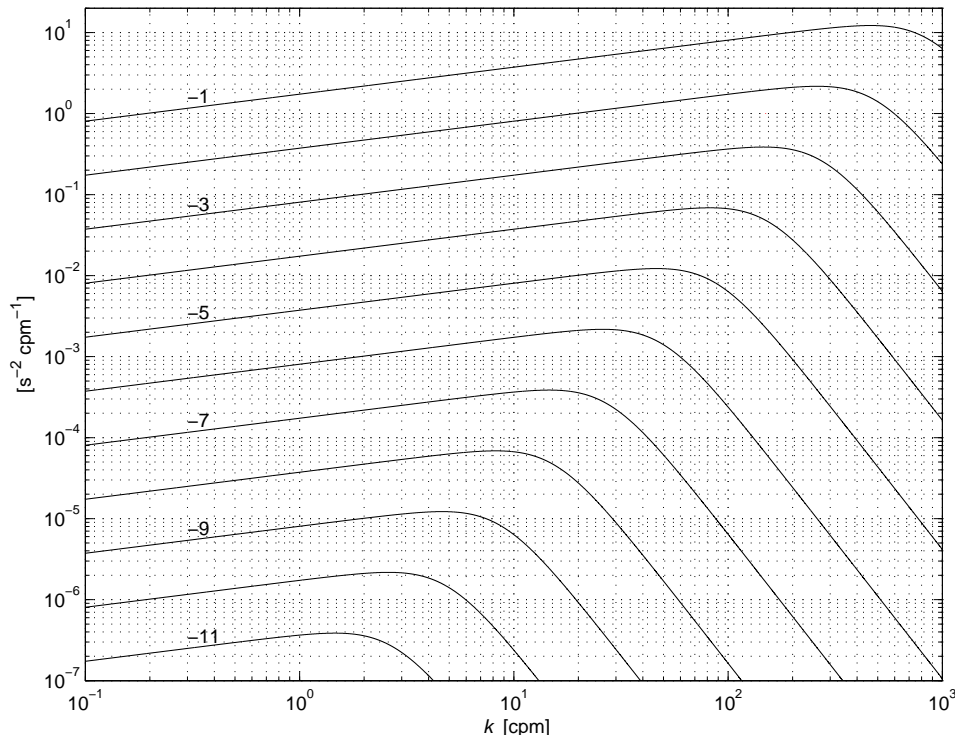


Figure 10: The dimensional Nasmyth spectrum for dissipation rates of 10^{-11} to 10^{-1} W kg^{-1} , and a kinematic viscosity of $\nu = 1 \times 10^{-6}$ $\text{m}^2 \text{s}^{-1}$. The vertical red line is at $k = 150$ cpm.

4.1 Exploiting the Nasmyth spectrum

The rate of dissipation of TKE has a very wide range in the ocean. The smallest reported values are $\sim 3 \times 10^{-11}$ W kg^{-1} measured over the deep abyssal plains while values up to $\sim 3 \times 10^{-2}$ W kg^{-1} have been observed in the outflow of Mediterranean water [11]. When we plot the Nasmyth spectrum in dimensional form (Figure 10), we see that the peak of the spectrum moves to higher wavenumbers in proportion to $\epsilon^{1/4}$ and that the peak moves up in proportion to $\epsilon^{3/4}$, which is a property that the spectrum must have in order for the rate of dissipation to be proportional to the integral of the spectrum.

If we look at the $+1/3$ range of the spectrum (the inertial subrange), then we see that, at any given wavenumber, the spectrum rises in proportion to $\epsilon^{2/3}$. This means that the integral of the spectrum to a limited wavenumber, say 10 cpm,

$$\epsilon_{10} = \frac{15}{2} \nu \int_0^{10} \Psi(k) dk \quad (7)$$

where Ψ is the measured shear spectrum, can provide a good initial estimate of the rate of dissipation. For large dissipation rates, the ratio ϵ/ϵ_{10} is proportional to $\epsilon^{1/3}$ (Figure 11). The problem is that we do not know the true dissipation rate ϵ . If we express the ratio ϵ/ϵ_{10} in terms of the ϵ_{10} , then we can predict the true dissipation rate quite accurately (Figure 12). For very low rates of dissipation, the ratio is close to 1 because by integrating to 10 cpm we have resolved nearly all shear variance. That is, $\epsilon_{10} \approx \epsilon$ when $\epsilon \lesssim 10^{-8}$ W kg^{-1} . For large

rates of dissipation, the ratio ϵ/ϵ_{10} grows in proportion to $\epsilon_{10}^{1/2}$. The simple mathematical model

$$\frac{\epsilon}{\epsilon_{10}} = \sqrt{1 + a\epsilon_{10}} \quad (8)$$

where $a = 1.0774 \times 10^9 \text{ kg W}^{-1}$ is accurate to 4% (Figure 13).

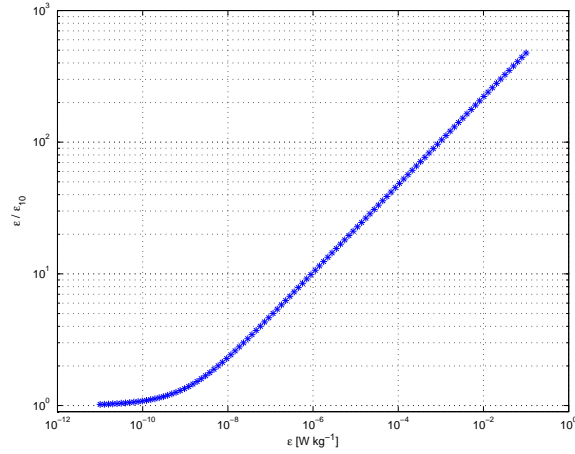


Figure 11: Ratio of true dissipation to that from integration to 10 cpm, ϵ/ϵ_{10} as a function of ϵ .

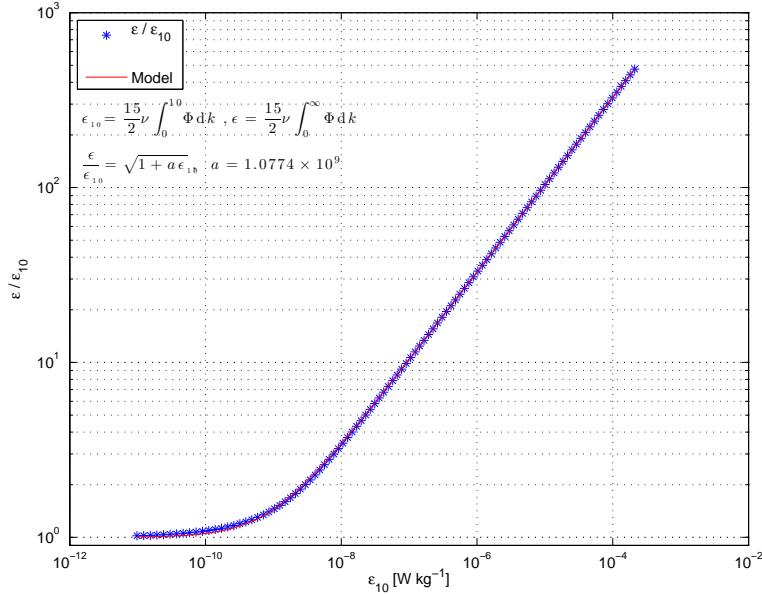
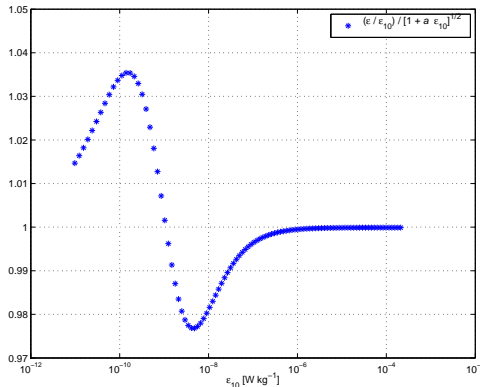


Figure 12: Ratio of true dissipation to that from integration to 10 cpm, ϵ/ϵ_{10} as a function of ϵ_{10} .

The initial estimate of the rate of dissipation, obtained from an integration of the shear spectrum to 10 cpm, can be used to guide the algorithm for estimating the rate of dissipation.

Figure 13: Quality of the fit of ϵ/ϵ_{10} to ϵ_{10} .

For example, it provides a good translation of the dimensional wavenumber into a non-dimensional wavenumber, which in turn can be used to estimate the fraction of the shear variance that is resolved at any dimensional wavenumber.

The initial estimate of the rate of dissipation can be used to choose between estimating the rate of dissipation by integrating the spectrum (the variance method) or, if the initial estimate is high, using a fit to the inertial subrange. For example, for an initial dissipation rate $\epsilon \gtrsim 10^{-5} \text{ W kg}^{-1}$ the rate of dissipation should be estimated from the level of the +1/3 range of the spectrum rather than from the variance of the spectrum, because the variance will not be well resolved.

The initial estimate can also be used to constrain the upper limit of integration. The measured spectra must be corrected for the spatial averaging by the shear probes (4), and it is not wise to extend the correction beyond 150 cpm (Figure 10, red line) because, at that wavenumber, the spectrum is boosted by a factor of 10.8. The dimensional wavenumber of 150 cpm can be translated into a non-dimensional wavenumber and this can be used to estimate the fraction of the variance that will be resolved by integration.

The initial estimate of the rate of dissipation can also be used to constrain the wavenumber range used by the algorithm that tries to find the spectral minimum (in order to determine the upper limit of integration). For example, there is little value in looking for a minimum beyond the wavenumbers that contain, say, more than 90% of the variance. At that wavenumber, the spectrum will have fallen about a factor of 10 below its peak. An erroneously high wavenumber for the spectral minimum will likely bias the estimate high by including noise.

4.1.1 Recursive estimation of ϵ

The initial, and the subsequently refined, estimates of the rate of dissipation can be used to estimate the fraction of the variance that is resolved, and then to adjust upwards the estimate to account for the missing variance. This adjustment must be applied recursively but it will converge very rapidly because the non-dimensional wavenumber scales with $\epsilon^{1/4}$. For

example, say that the actual rate of dissipation is $\epsilon = 1 \times 10^{-7} \text{ W kg}^{-1}$, $\nu = 1 \times 10^{-6} \text{ m}^2 \text{ s}^{-1}$, that the measured spectrum is identical to the dimensional Nasmyth spectrum, and that the algorithm decided to set the limit of integration to 30 cpm, which is barely above the peak of the spectrum (Figure 10). This is a very poor choice for the upper limit of integration and even our current algorithm seldom performs this poorly. Integration to 30 cpm gives an estimate of $\epsilon_0 = 0.71 \times 10^{-7} \text{ W kg}^{-1}$. The corresponding non-dimensional wavenumber is $x_0 = 30(\nu^3/\epsilon)^{1/4} = 0.0581$. According to the model of the integral of the Nasmyth spectrum (6), we have resolved 0.754 of the variance. Our new estimate of the rate of dissipation is then $\epsilon_1 = 0.71 \times 10^{-7}/0.754 = 0.94 \times 10^{-7} \text{ W kg}^{-1}$ – low by only 6%. In the next iteration we get $x_1 = 0.0542$, a resolved fraction of 0.718, and a new estimate of $\epsilon_2 = 0.71 \times 10^{-7}/0.718 = 0.99 \times 10^{-7} \text{ W kg}^{-1}$. No further iteration is required.

4.2 A note on integration

The shear spectrum is usually integrated using the trapezoidal-method. Zero wavenumber must be included in the integration. When the rate of dissipation is very small, or the lowest non-zero wavenumber in a spectrum is fairly large, it is possible to introduce a small error due to the method of integration. For the lowest wavenumbers, we can consider the spectrum to be proportional to $k^{1/3}$. True integration from wavenumbers 0 to k_1 , the first non-zero wavenumber of the spectrum, gives

$$\int_0^{k_1} k^{1/3} dk = \frac{3}{4} k_1^{4/3} \quad (9)$$

while the trapezoidal method gives only

$$\frac{1}{2} k_1^{4/3} . \quad (10)$$

The error gets smaller for the next interval because

$$\int_{k_1}^{2k_1} k^{1/3} dk = \frac{3}{4} (2^{4/3} - 1) k_1^{4/3} \quad (11)$$

while the trapezoidal method gives

$$\frac{1}{2} (2^{1/3} + 1) k_1^{4/3} \quad (12)$$

which is smaller by less than 1%. Thus, the estimate of the rate of dissipation may need to be adjusted upwards for the “missing” variance at the bottom end of the spectrum. One method is to estimate the rate without consideration to the bottom end, and then use this estimate to calculate the expected Nasmyth spectral value at the first non-zero wavenumber, k_1 . The missing variance is,

$$\frac{1}{4} k_1 \Psi(k_1) \quad (13)$$

where $\Psi(k_1)$ is the dimensional Nasmyth spectrum at wavenumber k_1 for the estimated rate of dissipation.

References

- [1] H. Tennekes and J. L. Lumley. *A First Course in Turbulence*. MIT Press, 1989.
- [2] A. N. Kolmogorov. Local structure of turbulence in an incompressible fluid at very high reynolds number. *Doklady AN SSSR*, 4:299–303, 1941.
- [3] P. W. Nasmyth. *Ocean Turbulence*. PhD thesis, University of British Columbia, Vancouver, British Columbia, Canada, 1970.
- [4] N. S. Oakey. Determination of the rate of dissipation of turbulent kinetic energy from simultaneous temperature and velocity shear microstructure measurements. *Journal of Physical Oceanography*, 12:256–271, 1982.
- [5] T. E. Siddon and H. S. Ribner. An aerofoil probe for measuring the transverse component of turbulence. *J. American Inst. Aeronautics and Astronautics*, 3:747–749, 1965.
- [6] T. E. Siddon. A miniature turbulence gauge for utilizing aerodynamic lift. *Review of Scientific Instruments*, 42:653–656, 1971.
- [7] T. R. Osborn and W. R. Crawford. An airfoil probe for measuring turbulent velocity fluctuations in water. In F. W. Dobson and R. Davis, editors, *Air-Sea Interaction: Instruments and Methods*, Mechanical Engineering, page 535. Plenum, 1980.
- [8] P. Macoun and R. Lueck. Modelling the spatial response of the airfoil shear probe using different sized probes. *Journal of Atmospheric and Oceanic Technology*, 21:284–297, 2004.
- [9] L. Goodman, E. R. Levine, and R. G. Lueck. On measuring the terms of the turbulent kinetic energy budget from an auv. *Journal of Atmospheric and Oceanic Technology*, 23:977–990, 2006.
- [10] F. Wolk, H. Yamazaki, L. Seuront, and R. G. Lueck. A new free-fall profiler for measuring bio-physical microstructure. *Journal of Atmospheric and Oceanic Technology*, 19:780–793, 2002.
- [11] J. F. Price, M. O. Baringer, R. G. Lueck, G. C. Johnson, I. Ambar, G. Parrilla, A. Cantos, M. A. Kennelly, and T. B. Sanford. Mediterranean outflow mixing dynamics. *Science*, 259:1277–1282, 1993.

End Of Document